The reactivity of complexes containing the $[Mo_3(\mu_3S)(\mu S_2)_3]^{4+}$ core. Ligand substitution, sulfur elimination and sulfide binding*

Marc D. Meienberger, Kaspar Hegetschweiler** and Heinz Rüegger
Laboratorium für Anorganische Chemie, ETH Zentrum, CH-8092 Zurich (Switzerland)

Volker Gramlich
Institut für Kristallographie und Petrographie, ETH Zentrum, CH-8092 Zurich (Switzerland)

(Received March 29, 1993)

Abstract

The reactivity of complexes, containing the $[Mo_3(\mu_3S)(\mu S_2)_3]^{4+}$ core, was investigated in solution. Three types of electrophilic centers, (i) the three Mo atoms, (ii) the three equatorial (in plane) and (iii) the three axial (out of plane) sulfur atoms of the disulfido bridges, interact distinctly different with nucleophilic agents. The selective reactivity enabled the specific synthesis of new complexes containing either the $[Mo_3(\mu_3S)(\mu S_2)_3]^{4+}$ or the $[Mo_3(\mu_3S)(\mu S)_3]^{4+}$ cores by using $(NEt_4)_2[Mo_3S(S_2)_3Br_6]$ as starting material. A combination of sulfur abstraction and ligand substitution resulted in the formation of complexes of the composition $[Mo_3S_4L_3]^{4+}$, where L represents the tridentate N,O donors 1,3,5-triamino-1,3,5-trideoxy-*cis*-inositol and 1,3,5-trideoxy-1,3,5-tris(dimethylamino)-*cis*-inositol. The complexes were characterized by one- and two-dimensional NMR spectroscopy and FAB mass spectrometry. In the presence of a weak base and 6-mercaptopurine (Hmp) or 8-hydroxyquinoline (Hoxq), the six Br atoms were replaced by these bidentate ligands forming $[Mo_3S(S_2)_3(oxq)_3]^+$ and $[Mo_3S(S_2)_3(mp)_3]^+$. In addition, the three oxq ligands could be quantitatively replaced by diethyldithiocarbamate (dtc^-) in the presence of a slight excess of Na(dtc). The $[Mo_3S(S_2)_3]^{4+}$ core was not affected under the harsh reaction conditions, but S^{2-} was liberated by hydrolysis of dtc^-. The formed S^{2-} anion was bound selectively to the three S_{ax} atoms of the $[Mo_3S(S_{eq}\text{–}S_{ax})_3]^{4+}$ core, resulting in the formation of the dimer $[Mo_3S(S_2)_3(dtc)_3]_2S$. The dimeric structure was established by X-ray analysis, exhibiting a hexacoordinated S^{2-} atom with a rather short average S_{ax}–S^{2-} distance of 2.71 Å and an elongated S_{eq}–S_{ax} distance of 2.11 Å. Space group *Aba*2, $a = 17.48(1)$, $b = 26.13(2)$, $c = 16.489(8)$ Å, $Z = 4$, $R = 0.051$.

Introduction

The growing interest in polynuclear chalcogenide complexes of molybdenum and tungsten resulted in the investigation of a variety of novel preparation methods for such compounds: excision of cluster cores from polymeric solids [1–3], substitution of peripheral ligands [4–8], degradation of polychalcogenide bridges [3], building-up of the cluster core from mononuclear [9] or dinuclear species [10], or fragmentation of a cluster unit of higher nuclearity [11]. In this context, the trinuclear $[Mo_3S(S_2)_3Br_6]^{2-}$ proved to be a useful intermediate for the preparation of further complexes of the $[Mo_3S(S_2)_3]^{4+}$ and $[Mo_3S_4]^{4+}$ cores. This was discovered at about the same time by Fedin *et al.* [12] and in our laboratory [4]. It has been shown that the $[Mo_3S(S_2)_3]^{4+}$ core is highly resistant against acids and oxidizing agents [4, 5, 12] (the oxidative fragmentation of $Mo_3S_7Br_4$ as described by Cotton *et al.* [13] is a remarkable exception), whereas it reacts easily with nucleophilic or reducing agents [3, 6, 14]. Three different types of interaction between the $[Mo_3S(S_2)_3]^{4+}$ core and nucleophilic agents are known (Scheme 1).

(a) The three disulfido groups can be degradated to monosulfido groups by sulfur-abstracting agents like PPh_3 or CN^- [3, 14]. Recent studies on the mechanism of this reaction revealed the selective elimination of the equatorial (in plane) sulfur atoms [12, 15]. The axial (out of plane) sulfur atoms are retained.

(b) An attack of the nucleophilic agent on the molybdenum atoms results in the substitution of the peripheral ligands. It has been shown that $[Mo_3S(S_2)_3Br_6]^{2-}$ reacts with monodentate and bidentate ligands under complete preservation of the $[Mo_3S(S_2)_3]^{4+}$ core. These experiments exhibited clearly a different lability of Br_{cis} and Br_{trans}: substitution with

*Part of this work was presented at the 29th International Conference on Coordination Chemistry, Lausanne, July 19–24, 1992.

**Author to whom correspondence should be addressed.

0020-1693/93/$6.00

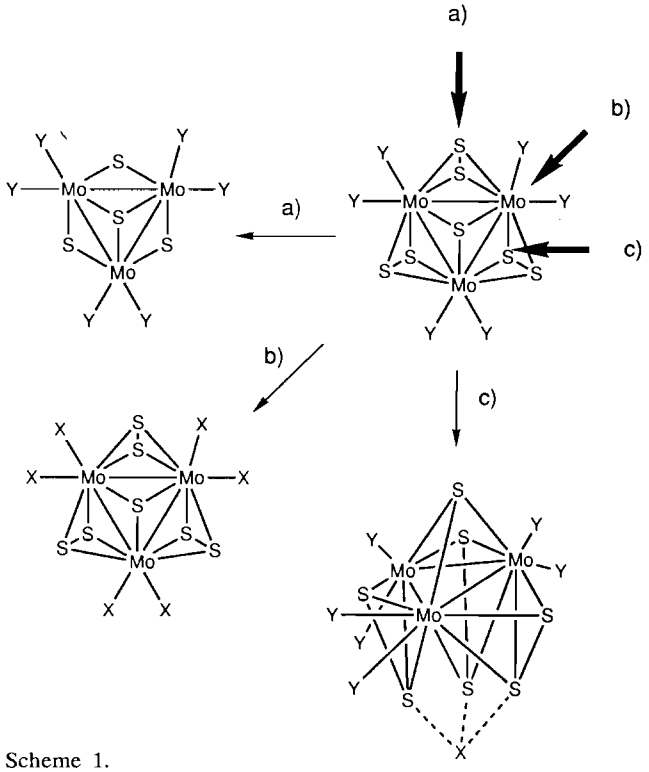

Scheme 1.

bidentate S, O donors resulted in the selective formation of one single stereoisomer with the oxygen donors in *trans* position [4, 6]. Furthermore, in the reaction with the monodentate aniline, only a substitution in the three *cis* positions has been observed [8].

(c) It has been recognized that the three axial (out of plane) sulfur atoms in the $[Mo_3S(S_2)_3]^{4+}$ core have a pronounced affinity to bind additional anions [5, 6, 8, 16–21]. This anion binding even occurs when the complex has a negative total charge as indicated by the equation $[Mo_3S(S_2)_3Cl_6]^{2-} + Cl^- \rightarrow [Mo_3S(S_2)_3Cl_6]Cl^{3-}$ [21]. However, in contrast to the above discussed reactivity of the equatorial sulfur atoms, no degradation of the bridging disulfido groups takes place.

The observed reactivity of the $[Mo_3S(S_2)_3]^{4+}$ complexes is understandable considering the electronic structure of such complexes. Müller *et al.* recently performed SCF-Xα calculations for $[Mo_3S_{13}]^{2-}$ ($=[Mo_3(\mu_3S)(\mu S_2)_3(S_2)_3]^{2-}$) [22]. These calculations revealed a positive net atomic charge on S_{eq} (+0.18) and S_{ax} (+0.27). Since a given nucleophile interacts obviously in a different way with the three types of electrophilic centers in the $[Mo_3S(S_2)_3]^{4+}$ core, a more comprehensive understanding of the reactivity of $[Mo_3S(S_2)_3]^{4+}$ complexes is necessary for an efficient design of novel synthetic pathways. In the present contribution, attention is therefore addressed to the following considerations.

(i) Is it possible to predict whether a selected nucleophile attacks the $[Mo_3S(S_2)_3]^{4+}$ core on the Mo, S_{eq} or S_{ax} atom?

(ii) Is it possible to govern this selectivity by use of different peripheral ligands?

(iii) Since the peripheral ligands of $[Mo_3S(S_2)_3Br_6]^{2-}$ are particularly labile, a combination of ligand substitution and sulfur elimination opens a wide range of synthetic applications. The present contribution establishes this pathway and confirms that $[Mo_3S(S_2)_3Br_6]^{2-}$ is a versatile and convenient synthon for the preparation of novel complexes containing either the $[Mo_3S(S_2)_3]^{4+}$ or the $[Mo_3S_4]^{4+}$ core.

Experimental

Physical measurements and analyses

UV–Vis spectra were recorded on an Uvikon 940 spectrophotometer, NMR spectra were recorded on Bruker AC-200 (^{1}H at 200.13 MHz) and AMX-500 (500.13 and 125.9 MHz for ^{1}H and ^{13}C, respectively) spectrometers. 2D NMR experiments (COSY [23], TOCSY [24] and ^{13}C,^{1}H-HMQC [25]) were performed according to the literature. Chemical shifts (δ, ppm) are given relative to (trimethylsilyl)propionate-d^4 (=0 ppm). C, H and N analyses were performed by D. Manser, Laboratorium für Organische Chemie, ETH Zürich, Mo was determined photometrically as bis(tironato)molybdenum(VI) (390 nm) after digestion of the sample by aqua regia. Karl Fischer titrations were used to determine the H_2O content of DMSO-d^6.

Synthetic work

All reactions were carried out in air. CH_2Cl_2, DMF, EtOH, CH_3CN, NEt_3, PPh_3, sodiumdiethyldithiocarbamate trihydrate (=Na(dtc)·3H$_2$O) and 6-mercaptopurine (=Hmp·H$_2$O) were commercially available compounds of usual reagent grade quality. They were used without further purification. $(NEt_4)_2[Mo_3S(S_2)_3Br_6]$ [4], $[Mo_3S(S_2)_3(oxq)_3]Br$ (Hoxq=8-hydroxyquinoline) [5], 1,3,5-triamino-1,3,5-trideoxy-*cis*-inositol (=taci) [26] and 1,3,5-trideoxy-1,3,5-tris(dimethylamino)-*cis*-inositol (=tdci) [27] were synthesized as described previously. A solution of the $[Mo_3S_4]^{4+}$ aqua ion was prepared following the method given by Cotton *et al.* [28].

$[Mo_3S_4(tdci)_3]Br_4$ (1)

420 mg (0.335 mmol) of $(NEt_4)_2[Mo_3S_7Br_6]$ were dissolved in 100 ml of boiling CH_3CN. The addition of 770 mg (2.95 mmol) of solid tdci resulted in the precipitation of a yellow solid. 264 mg (1.01 mmol) solid PPh_3 were then added and the suspension was kept under reflux for an additional 2 h. A color change

from yellow to green was observed. The suspension was filtered and the deep green solution was evaporated to dryness and redissolved in 100 ml of H_2O. The solution was allowed to stand at 4 °C for 24 h and solid $SPPh_3$ was removed by filtration. The solution was then evaporated to dryness again. The solid residue was dissolved in EtOH and layered with hexane, resulting in green crystals of **1** which effloresced immediately in air. *Anal.* Calc. for the dried product: $C_{36}H_{81}Br_4Mo_3N_9O_9S_4$: C, 28.45; H, 5.37; N, 8.29; Mo, 18.94. Found: C, 28.45; H, 5.57; N, 8.19; Mo, 19.02%. NMR: see Table 1.

Cu complex (2)

A total of 50 mg of solid **1** was dissolved in 20 ml of EtOH. 1 g of elemental Cu was then added and the suspension was stirred for 1 h at room temperature. The excess of Cu was filtered off and the resulting brown solution was layered with hexane, resulting in deep reddish brown crystals.

$[H_{-2}Mo_3S_4(taci)_3]Br_2$ (3)

437 mg (2.47 mmol) of taci were dissolved in 300 ml of boiling EtOH. Further addition of 772 mg (0.62 mmol) of solid $(NEt_4)_2[Mo_3S(S_2)_3Br_6]$ resulted in the precipitation of a pale yellow solid. The suspension was kept under reflux for 2 h and 485 mg (1.85 mmol) of PPh_3 were added. The solution was refluxed for an additional 3 h and a deep green solid was filtered off. The solid was dissolved in 150 ml of water and allowed to stand for 24 h at 4 °C. Some precipitated $SPPh_3$ was removed by filtration and the deep green solution was evaporated to a total volume of 20 ml. The solution was layered with acetone resulting in the formation of green crystals. *Anal.* Calc. for $C_{18}H_{43}N_9O_9S_4Mo_3Br_2 \cdot 3H_2O \cdot 2.5C_3H_6O$: C, 23.47; H, 4.94; N, 9.66. Found: C, 23.36; H, 4.91; N, 9.66% (the presence of 2.5 equiv. of acetone was confirmed by the NMR spectrum).

$[Mo_3S_7(dtc)_3]_2S$ (4)

12 mg (11.71 μmol) of $[Mo_3S(S_2)_3(oxq)_3]Br$ were dissolved in 1 ml of wet DMSO-d^6 (content of H_2O: 0.25%). 8 mg (35.5 μmol) of $Na(dtc) \cdot 3H_2O$ were then added and the brown–red solution was heated in an NMR tube (100 °C) over a period of 50 h. Brown crystals were formed, which were separated from the mother liquor, washed with CH_2Cl_2 and dried in air. They were suitable for single crystal X-ray diffraction experiments. *Anal.* Calc. for $C_{30}H_{60}N_6S_{27}Mo_6$: C, 18.51; H, 3.11; N, 4.32. Found: C, 18.71; H, 3.01; N, 4.36%.

$[Mo_3S(S_2)_3(mp)_3]Br$ (5)

554 mg (0.44 mmol) of $(NEt_4)_2[Mo_3S(S_2)_3Br_6]$ and 1.334 g (7.84 mmol) of $Hmp \cdot H_2O$ were dissolved in 80 ml of hot DMF (100 °C). 682 mg of NEt_3, dissolved in 15 ml of DMF, were added dropwise to the solution within 5 min. A color change from orange to deep red was noted and a brown solid precipitated. The suspension was allowed to stand at 100 °C for 1 h. The solid was then filtered off and the excess of Hmp was removed by soxhlet extraction (MeOH, 3d). The final product was washed with Et_2O and dried *in vacuo*. *Anal.* Calc. for $C_{15}H_9N_{12}S_{10}BrMo_3$: C, 17.23; H, 0.87; N, 16.07; Mo, 27.52. Found: C, 17.49; H, 1.38; N, 15.89; Mo, 26.9%.

FAB mass spectrometry

Mass spectra were measured on a VG ZAB VSEQ double-focusing mass spectrometer equipped with a VG-Cs-Ion FAB gun (35 keV, 2 μA beam current). Positive ion detection was used for all spectra. The samples were dissolved in a suitable solvent (**1**, **2** and **3**: H_2O; **4** and **5**: DMF) and mixed with the matrix (**1**, **2** and **3**: glycerol; **4** and **5**: 3-nitrobenzyl alcohol). Assignments are based on the analysis of the isotope pattern including all isotopes of C, H, N, O, S, Cu, Mo, Br with natural abundance $\geq 0.001\%$. Ion overlap was analyzed by least-squares calculations [29] $Ad - p = r$, $r^2 =$ minimum, where A is the $M \times N$ abundance matrix, which contains the contribution of each isotopic species at each mass, d is the vector of the calculated amounts of the N species, p is the vector of the M measured intensities, and r is the vector of the residuals. The goodness of fit was checked by an unweighted reliability factor $R = \Sigma|r_i|/\Sigma|p_i|$. The MS measurements are sum-

TABLE 1. ^1H and ^{13}C NMR data of $[Mo_3S_4(tdci)_3]^{4+}$ (D_2O, pH 9.5, room temperature)

Assignment[a]	$\delta(H)_{complex}$	$\delta(H)_{ligand}$	$\Delta\delta(H)$[b]	$\delta(C)_{complex}$	$\delta(C)_{ligand}$	$\Delta\delta(C)$[b]
HC(1)–N–Mo	2.95	2.43	0.52	77.2	68.4	8.8
HC(2)–O–Mo	5.31	4.67	0.64	72.2	67.7	4.5
HC(3)–N	2.81	2.43	0.38	69.2	68.4	0.8
HC(4)–O	4.48	4.67	−0.19	66.5	67.7	−1.2
CH_3–N–C(1)	3.82	2.61	1.21	59.0	44.6	14.4
CH_3–N–C(3)	2.83	2.61	0.23	44.0	44.6	−0.6

[a]The numbering scheme for the carbon atoms in coordinated tdci is given in Scheme 2. [b]$\Delta\delta = \delta_{complex} - \delta_{ligand}$.

TABLE 2. Summarized MS data

Compound	Ion	Intensity (%)
1	$[Mo_3S_4(tdci)_3-2H]^{2+}$	47
	$[Mo_3S_4(tdci)_2(H_2O)-3H]^+$	17
	$[Mo_3S_4(tdci)_2Br-2H]^+$	10
	$[Mo_3S_4(tdci)_3-3H]^+$	100
2	$[Mo_3S_4(tdci)_3-3H]^+$	80
	$[CuMo_3S_4(tdci)_3-4H]^+$	100
	$[CuMo_3S_4(tdci)_3(H_2O)]^+$	95
	$[Cu_2Mo_3S_4(tdci)_3-5H]^+$	57
	$[Cu_2Mo_3S_4(tdci)_3(H_2O)-2H]^+$	56
3	$[Mo_3S_4(taci)_2(H_2O)-3H]^+$	28
	$[Mo_3SO_3(taci)_3-3H]^+$	6
	$[Mo_3S_2O_2(taci)_3-3H]^+$	16
	$[Mo_3S_3O(taci)_3-3H]^+$	42
	$[Mo_3S_4(taci)_3-3H]^+$	100
4	$[Mo_3S_6(dtc)_3]^+$	20
	$[Mo_3S_7(dtc)_3]^+$	100
5	$[Mo_3S_4(mp)_3]^+$	19
	$[Mo_3S_5(mp)_3]^+$	24
	$[Mo_3S_6(mp)_3]^+$	28
	$[Mo_3S_7(mp)_3]^+$	100
	$[Mo_3S_7(mp)_3HBr]^+$	19

TABLE 3. Crystallographic data for $[Mo_3S(S_2)_3(dtc)_3]_2S$

Chemical formula	$C_{30}H_{60}N_6Mo_6S_{27}$
Formula weight	1946.2
Crystal size (mm)	0.1×01.×0.06
Space group	*Aba*2 (No. 41)
a (Å)	17.48(1)
b (Å)	26.13(2)
c (Å)	16.489(8)
V (Å^3)	7529(9)
Z	4
D_{calc} (g/cm^3)	1.72
μ(Mo Kα) (cm^{-1})	17.51
Temperature (°C)	20
R^a	0.051
$R_w{}^b$	0.051

$^aR=\Sigma||F_o|-|F_c||/\Sigma|F_o|$. $^bR_w=[\Sigma w(|F_o|-|F_c|)^2/\Sigma w|F_o|^2]^{1/2}$, $w=1/\sigma^2(|F_o|)$.

marized in Table 2. $R \leqslant 0.15$ was observed for all assignments.

Single crystal X-ray diffraction studies

Crystallographic data of $[Mo_3S(S_2)_3(dtc)_3]_2S$ are summarized in Table 3. A total of 2584 reflections was collected on a Syntex P21 four circle diffractometer using graphite-monochromatized Mo Kα radiation (λ = 0.71073 Å). 2041 reflections were observed with $I \geqslant 2\sigma(I)$. The data were corrected for Lorentz and polarization effects. An absorption correction was not performed. The structure was solved in the space group *Aba*2 by the Patterson interpretation routine of SHELXTL PLUS (VMS) [30]. The positions of all non-hydrogen atoms of the $[Mo_3S_7(dtc)_3]_2S$ molecule were located and refined by a series of alternating difference electron syntheses and full-matrix least-squares refinements. The positions of 30 hydrogen atoms were calculated (riding model) and included in the refinement. A total of 221 parameters was varied, using anisotropic displacement parameters for the Mo and S atomic positions, and isotropic displacement parameters for the N and C positions (R = 6.48%, R_w = 7.72%). The remaining peaks Q(1): x = 0.659, y = 0.035, z = 0.286, Q(2): x = 0.638, y = −0.002, z = 0.228, Q(3): x = 0.602, y = 0.027, z = 0.356 and Q(4): x = 0.711, y = −0.024, z = 0.273, with electron densities between 2.4 and 1.3 e Å^{-3}, together with some weaker peaks, indicated the presence of an additional small molecule. However, it was not possible to find a chemically sensible model for these peaks. Assuming the presence of a highly disordered DMSO (= solvent) molecule, Q(1) was refined as sulfur and Q(2) as oxygen atom; Q(3) and Q(4) were refined as carbon atoms, using isotropic displacement parameters and occupancy factors of 0.5 for all four positions. A total of 237 parameters was used in the final full-matrix, least-squares refinement. The maximal and mean shift/e.s.d. were 0.061 and 0.004, the maximum and minimum in the final difference Fourier synthesis were 0.88 and −0.71 e Å^{-3}. The final atomic coordinates are presented in Table 4.

Results

Abbreviations for the ligands are summarized below.

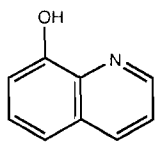

Hoxq

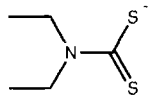

dtc$^-$

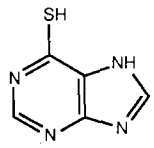

Hmp

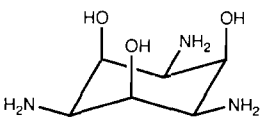

taci

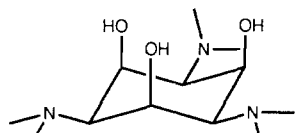

tdci

Preparation and characterization of $[Mo_3S_4(tdci)_3]^{4+}$

This complex was prepared according to the equation

$$[Mo_3S_7Br_6]^{2-} + 3PPh_3 + 3tdci \longrightarrow [Mo_3S_4(tdci)_3]^{4+} + 6Br^- + 3S{=}PPh_3$$

TABLE 4. Atomic coordinates and isotropic or equivalent isotropic displacement parameters with e.s.d.s in parentheses for non-hydrogen atoms of $[Mo_3S(S_2)_3(dtc)_3]_2S$

Atom	x	y	z	U_{eq}/U_{iso}[a] (Å^2)
Mo(1)	0.0194(1)	0.3797(1)	−0.1512(2)	0.037(1)
Mo(2)	0.0296(1)	0.3491(1)	0.0057(1)	0.038(1)
Mo(3)	−0.1092(1)	0.3717(1)	−0.0596(2)	0.037(1)
S	0	0.5	0.0005(6)	0.055(3)
S(1)	0.0522(3)	0.3287(2)	−0.2733(4)	0.050(2)
S(2)	0.0808(4)	0.4368(2)	−0.2564(4)	0.056(2)
S(3)	0.0739(4)	0.2659(2)	0.0625(4)	0.052(2)
S(4)	0.1091(4)	0.3635(2)	0.1319(4)	0.052(2)
S(5)	−0.2221(3)	0.3152(2)	−0.0836(4)	0.051(2)
S(6)	−0.2314(3)	0.4179(2)	−0.0244(4)	0.059(3)
S(7)	0.1412(3)	0.3517(3)	−0.0868(4)	0.049(2)
S(8)	−0.1108(3)	0.3946(2)	−0.2045(3)	0.046(2)
S(9)	−0.0926(3)	0.3355(2)	0.0797(4)	0.050(2)
S(10)	0.0942(3)	0.4231(2)	−0.0493(4)	0.048(2)
S(11)	−0.0677(3)	0.4499(2)	−0.1232(3)	0.046(2)
S(12)	−0.0583(3)	0.4115(2)	0.0606(3)	0.046(2)
S(13)	−0.0306(3)	0.3014(2)	−0.0989(3)	0.039(2)
C(11)	0.0860(11)	0.3831(9)	−0.3150(14)	0.044(6)
N(1)	0.1084(11)	0.3851(7)	−0.3944(11)	0.062(6)
C(12)	0.1083(14)	0.3373(9)	−0.4464(15)	0.069(8)
C(13)	0.1268(15)	0.4348(10)	−0.4361(17)	0.083(9)
C(14)	0.1754(14)	0.3064(10)	−0.4342(17)	0.085(9)
C(15)	0.2041(16)	0.4418(12)	−0.4461(22)	0.146(14)
C(21)	0.1179(12)	0.2998(8)	0.1386(13)	0.044(6)
N(2)	0.1568(9)	0.2760(6)	0.1976(10)	0.039(4)
C(22)	0.1995(13)	0.3066(9)	0.2556(14)	0.065(7)
C(23)	0.1577(13)	0.2199(8)	0.2009(15)	0.060(7)
C(24)	0.1515(13)	0.3183(9)	0.3315(16)	0.087(9)
C(25)	0.2286(14)	0.1963(9)	0.1629(15)	0.076(9)
C(31)	−0.2787(11)	0.3653(8)	−0.0558(14)	0.045(6)
N(3)	−0.3564(9)	0.3627(7)	−0.0599(12)	0.050(5)
C(32)	−0.3972(15)	0.3203(9)	−0.0986(14)	0.070(8)
C(33)	−0.4034(16)	0.4061(10)	−0.0292(16)	0.080(9)
C(34)	−0.4162(15)	0.3294(10)	−0.1871(16)	0.087(9)
C(35)	−0.4097(18)	0.4038(12)	0.0623(18)	0.107(11)

[a] $U_{eq} = \frac{1}{3}\Sigma_i\Sigma_j U_{ij} a^*_i a^*_j \mathbf{a}_i \mathbf{a}_j$.

The complex could be isolated as a crystalline compound of composition $[Mo_3S_4(tdci)_3]Br_4$, containing additional solvent of crystallization. X-ray analysis of the triclinic crystals (space group $P\bar{1}$, unit cell: $a = 15.46(2)$, $b = 17.29(4)$, $c = 18.48(1)$ Å, $\alpha = 103.7(1)$, $\beta = 102.23(9)$, $\gamma = 102.9(1)°$) revealed the presence of two $[Mo_3S_4(tdci)_3]Br_4$ entities in the unit cell ($Z = 2$). The $[Mo_3S_4X_9]$ unit (X = N, O) together with the 4 Br^- counter-ions could unambiguously be localized in the electron density map (Mo–Mo distances: 2.78(3), 2.82(2), 2.81(3) Å). However, the crystals were very fragile and effloresced immediately in air. They even decomposed slowly in their mother liquor in a glass capillary. A complete crystal structure analysis was therefore not possible. Thus, the formation of the $[Mo_3S_4(tdci)_3]^{4+}$ complex was established by spectroscopic methods and by the investigation of its chemical reactivity.

FAB mass spectrometry proved to be a particularly useful method in identifying the $[Mo_3S_4(tdci)_3]^{4+}$ unit. To understand the spectrum, it is crucial to recognize that each of the three coordinated ligands has three ionizable protons. Thus, the entire $[Mo_3S_4(tdci)_3]^{4+}$ complex must be regarded as a reservoir of a total of 9 ionizable protons, allowing any charge adjustment over a wide range. As a consequence, the entire complex can be observed in the form of the two ions $[Mo_3S_4(tdci)_3 - 3H]^+$ ($m/z = 1196.1$) and $[Mo_3S_4(tdci)_3 - 2H]^{2+}$ ($m/z = 598.3$) (Fig. 1). The observation of a dipositive species in the mass spectrum is well established for proteins but rather unusual for low molecular weight compounds.

The presence of the $[Mo_3S_4]^{4+}$ core is also indicated by the typical green colour which originates from a broad band in the Vis spectrum with a maximum at about 650 nm (Fig. 2). These spectroscopic properties did not change significantly in the range $5 \leqslant pH \leqslant 9$.

The ^1H NMR data of $[Mo_3S_4(tdci)_3]^{4+}$ (Table 1) showed 2 signals in a 6:12 ratio for the six methyl groups and 4 signals for the six ring protons in a 1:2:2:1 ratio, indicating the predominance of one stereoisomer. Because the ligand symmetry is therefore recognized to be C_v, C_{3v} is implied for the entire complex. Four possible sites of coordination (see Scheme 2) are conceivable, which would result in N_3, N_2O, NO_2 and O_3 coordination modes. The former two are excluded because of the observation of the W-type long-range couplings between the hydrogens assigned to be adjacent to OH groups. Such couplings are typical for equatorial hydrogens. The NO_2 coordination mode is implied by the characteristics of the ^{13}C NMR spectrum (see Table 1), which has been assigned by $^{13}C,^1H$ heteronuclear correlation. Thus, downfield shifts with respect to the free ligand ($\Delta\delta$), which are attributed to metal coor-

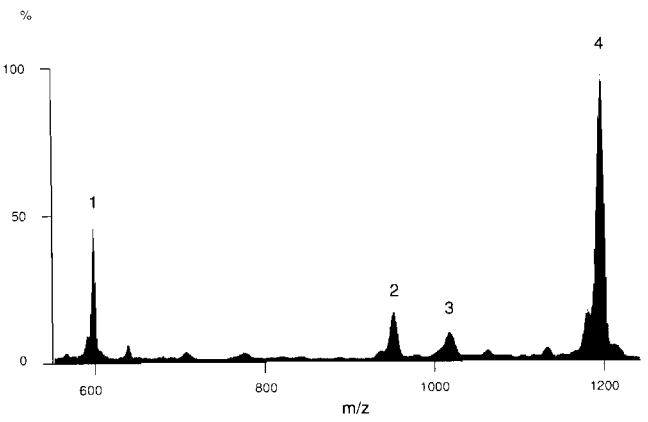

Fig. 1. FAB$^+$ mass spectrum of $[Mo_3S_4(tdci)_3]Br_4$ (H_2O, glycerol matrix). (1) $[Mo_3S_4(tdci)_3 - 2H]^{2+}$, (2) $[Mo_3S_4(tdci)_2(H_2O) - 3H]^+$, (3) $[Mo_3S_4(tdci)_2Br - 2H]^+$, (4) $[Mo_3S_4(tdci)_3 - 3H]^+$.

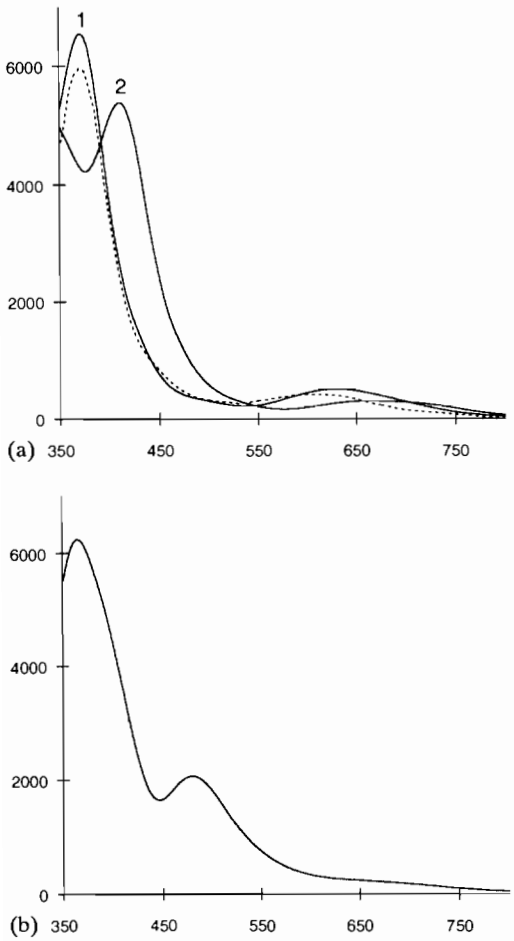

Fig. 2. (a) Vis spectrum of $[Mo_3S_4(taci)_3]Br_4$ (1), $[Mo_3S_4(tdci)_3]Br_4$ (2) and $[Mo_3S_4(H_2O)_9]^{4+}$ (dotted line). (b) Vis spectrum of $[Mo_3S_4(tdci)_3CuBr]$.

dination of the adjacent heteroatom are observed for C(1) and the methyl groups on the coordinated nitrogen and to a lesser extent for the C(2) carbon (Scheme 2). It should also be noted that the hydrogen on C(2) experiences a large downfield shift in this coordination mode.

Further evidence for the presence of the postulated $[Mo_3S_4(tdci)_3]^{4+}$ complex was obtained by the observation that the same complex was formed by treating the well known aqua ion $[Mo_3S_4(H_2O)_9]^{4+}$ with tdci in H_2O. Products with identical Vis and FAB^+ spectra were obtained, starting either from $[Mo_3S_4(H_2O)_9]Cl_4$ or $(NEt_4)_2[Mo_3S(S_2)_3Br_6]$. In addition $[Mo_3S_4(tdci)_3]^{4+}$ reacts in the presence of elemental Cu to the cubane-type cluster $[Mo_3S_4Cu(tdci)_3]^+$ [31]. The Cu containing compound, which we formulate as $[(Mo(tdci))_3(\mu_3S)_4CuBr]$ could be isolated in the form of deep brown crystals. Unfortunately, these crystals suffer from a similar instability as the above-mentioned $[Mo_3S_4(tdci)_3]Br_4$. However, the Mo_3S_4Cu unit could readily be identified in the mass spectrum by the

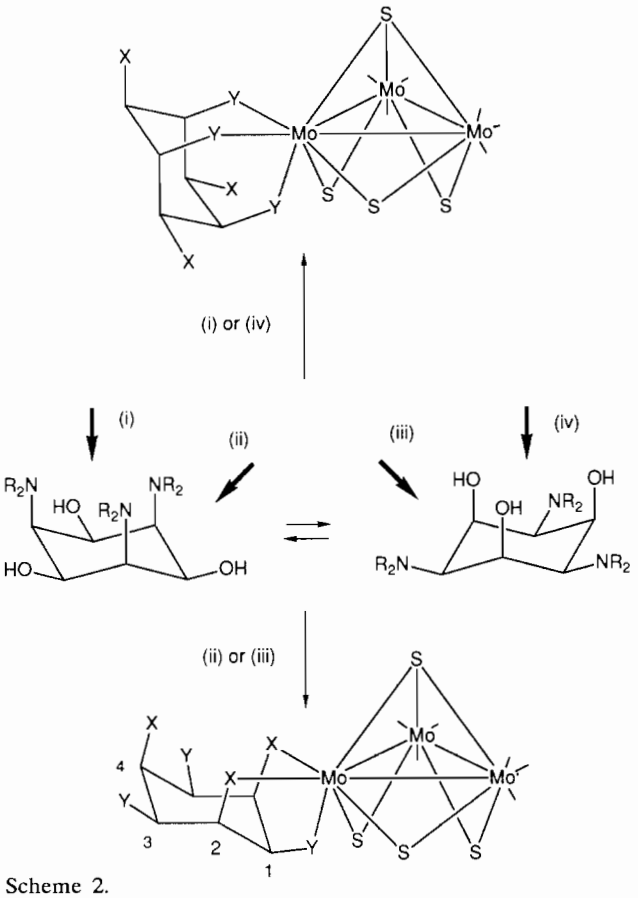

Scheme 2.

observation of the ions $[Mo_3S_4Cu(tdci)_3-4H]^+$ and $[Mo_3S_4Cu(tdci)_3(H_2O)]^+$ (Fig. 3 and Table 2).

Preparation and characterization of $[Mo_3S_4(taci)_3]^{4+}$

To confirm that $[Mo_3S(S_2)_3Br_6]^{2-}$ serves as a suitable intermediate for the synthesis of Mo_3S_4-type complexes, $[Mo_3S(S_2)_3Br_6]^{2-}$ was also allowed to react with the unmethylated taci. Since no solvent was able to dissolve both taci and $(NEt_4)_2[Mo_3S(S_2)_3Br_6]$ in a sufficient amount, the reaction was carried out in suspension. The resulting complex was very soluble in slightly acidic aqueous solution. However, the complex could be crystallized as $[H_{-2}Mo_3S_4(taci)_3]Br_2$ at $pH \approx 8$ by the addition of acetone. The formation of $[Mo_3S_4(taci)_3]^{4+}$ in the deep green solution could be unambiguously established from the FAB mass spectrum, (Table 2, Fig. 4). Again, an identical complex was obtained by using the aqua ion $[Mo_3S_4(H_2O)_9]^{4+}$ and an excess of taci as starting material. It is interesting to note that a series of signals $[M^+-16]^+$, $[M^+-32]^+$ and $[M^+-48]^+$ was observed in the spectrum of $[Mo_3S_4(taci)_3]^{4+}$ (Fig. 4). It seems reasonable to formulate these ions as $[Mo_3S_3O(taci)_3-3H]^+$, $[Mo_3S_2O_2(taci)_3-3H]^+$ and $[Mo_3SO_3(taci)_3-3H]^+$. The conversion $\mu_2S \rightarrow \mu_2O$ for $[Mo_3S_{4-x}O_x(H_2O)_9]^{4+}$,

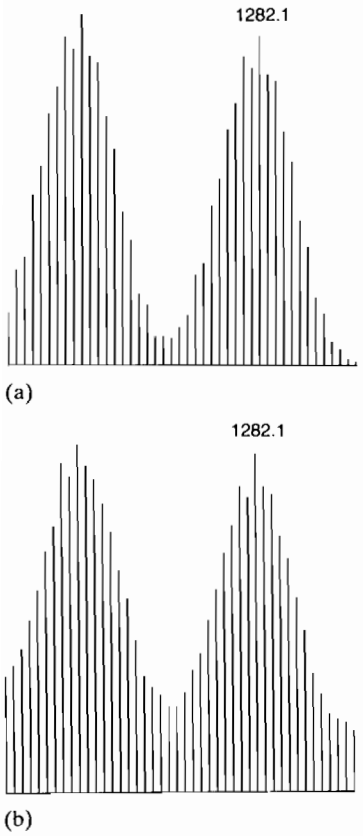

Fig. 3. (a) Calculated isotope distribution for the superposition of $[Mo_3S_4(tdci)_3Cu-4H]^+$ (100%) and $[Mo_3S_4(tdci)_3Cu(H_2O)]^+$ (95%). (b) Observed pattern in the FAB^+ mass spectrum of $[Mo_3S_4(tdci)_3CuBr]$. $R=0.149$.

$1 \leqslant x \leqslant 3$, has recently been established to occur in aqueous solution in the presence of a reducing agent [32]. It has been postulated that the prime process is a reduction of Mo(IV) to Mo(III) followed by a labilization and replacement of μ_2S by μ_2O. Thus the observation of these species in the FAB^+ mass spectrum of $[Mo_3S_4(taci)_3]^{4+}$ is quite reasonable as it is well known that glycerol can react as a reducing agent under FAB conditions. In particular metal ions are readily reduced as indicated by the observation of $[Zn(taci)]^+$ or $[Cd(taci)]^+$ in the spectrum of $Zn(taci)_2Br_2$ [33] or $Cd(taci)_2(NO_3)_2$ [34], respectively.

The ^1H NMR spectrum of $[Mo_3S_4(taci)_3]^{4+}$ in D_2O (pH 8) is exceedingly complicated due to the presence of four coordination modes of the taci ligand and its orientation relative to the Mo_3S_4 cluster core (Scheme 2). A TOCSY (total correlation spectroscopy) experiment, from which a representative section is shown in Fig. 5, proved helpful, as it allowed to group the taci ^1H resonances according to different modes of coordination. A structural assignment on the proton characteristics was, however, not possible and relies mostly on the interpretation of the carbon NMR parameters. Table 5 presents a relevant selection of ^{13}C

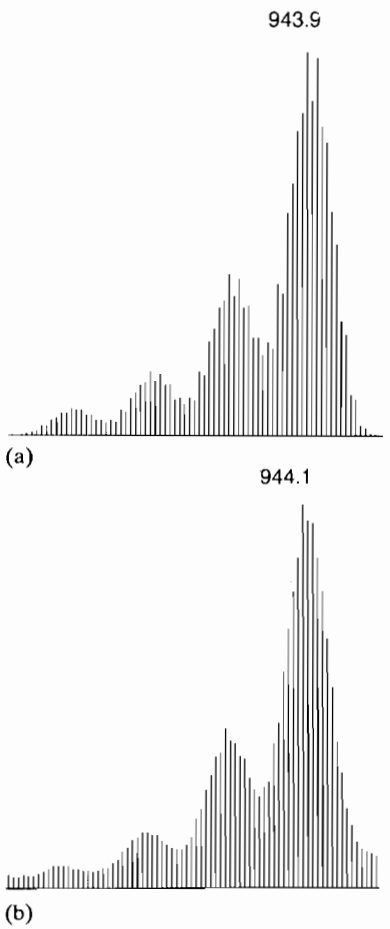

Fig. 4. (a) Calculated isotope distribution for the superposition of $[Mo_3O_3S(taci)_3-3H]^+$ (6%), $[Mo_3O_2S_2(taci)_3-3H]^+$ (16%), $[Mo_3OS_3(taci)_3-3H]^+$ (42%) and $[Mo_3S_4(taci)_3-3H]^+$ (100%). (b) Observed pattern in the FAB^+ mass spectrum of $[Mo_3S_4(taci)_3Br_4]$. $R=0.079$.

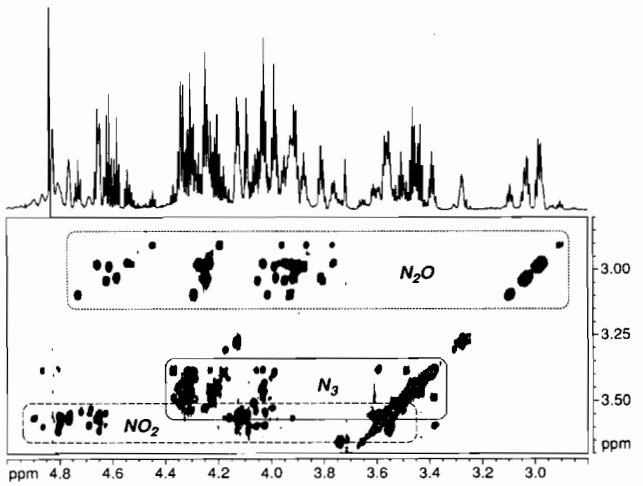

Fig. 5. Section of the ^1H TOCSY spectrum for $[Mo_3S_4(taci)_3]^{4+}$ (D_2O, pH 8, r.t., 11.4 Tesla, 150 ms MLEV-17 mixing with $\gamma/2\pi B_1 \approx 8.6$ KHz) with the conventional ^1H NMR spectrum plotted above. The three major coordination types are indicated.

TABLE 5. ^{13}C NMR data of model taci complexes[a]

Metal	O_3		NO_2				N_2O		N_3		Ref.
	δC(N)	δC(O)	δC(N)		δC(O)		δC(N)	δC(O)	δC(N)	δC(O)	
Al^{3+}	55.5	*71.6*									35
Ga^{3+}	56.0	*73.1*							*58.1*	67.7	35
Ge^{4+}	54.6	*75.1*									36
Co^{3+}									*52.1*	65.8	26
			52.2,	*64.7*	70.2,	*74.9*			*51.8, 52.2*	66.3, 65.9	37
			53.2,	*67.4*	71.0,	*74.9*					37
							63.4, *66.8*	72.8, *87.0*			37
Ti^{4+}	54.0	*72.7*									36
Sn^{4+}	56.2	*76.2*									36
Pb^{2+}				*62.4*		*75.8*					38
Bi^{3+}				*60.5*		*80.2*					38
Cd^{2+}									*57.6*	69.9	34
Tl^{3+}									*61.6*	67.9	35
Zn^{2+}									*57.1*	69.9	33
Average	55.3(9)	*73.8(18)*	52.7(4),	*63.8(26)*	70.6(4),	*76.5(22)*	63.4, *66.8*	72.8, *87.0*	*55.8(35)*	67.7(16)	

[a]Shifts printed in italics correspond to a carbon adjacent to a coordinating heteroatom. Chemical shifts for the free ligand are 77.7 and 54.9 ppm in the triamine form and 68.5 and 53.3 ppm for the triammonium form, respectively.

NMR data of model taci complexes whose structures have been ascertained by X-ray analysis.

Although there is only one reference example for an N_2O type coordinated taci, its lowest field carbon signal position is unparalleled and we tentatively assign the group of highly deshielded carbons in the *c.* 85 ppm range (Fig. 6) to the CH–O–Mo groups in this coordination mode. This deduction is supported in that the related protons are (i) significantly displaced towards lower field with respect to the free ligand, and (ii) well resolved into triplets, a common feature of axially positioned hydrogens. The remaining ^{13}C and ^{1}H resonances for this type are found from the combination of COSY, TOCSY and $^{13}C,^{1}H$ correlation experiments. Their shift positions are in agreement with the assignment to an N_2O coordination mode.

The NO_2 coordination mode, which was found to predominate in the case of the tdci ligand, is characterized by the largest deshielding of the hydrogens adjacent to the coordinated oxygens. The two proton resonances found in this region of the spectrum have a broad appearance and show in the COSY spectrum cross peaks due to mutual long-range couplings of the W-type, characteristic of equatorial protons. The corresponding ^{13}C chemical shifts in the range of *c.* 76 ppm and those of the carbons adjacent to the coordinated nitrogens at *c.* 62 ppm are all in accord with the N_2O coordination mode.

The third of the major types of taci coordination exhibits considerably less dispersion of the proton chemical shifts as can be seen from the TOCSY spectrum (Fig. 5). Furthermore, carbon chemical shifts (*c.* 68 and 53 ppm) for this type are found to be relatively close to those of the free ligand in its protonated form

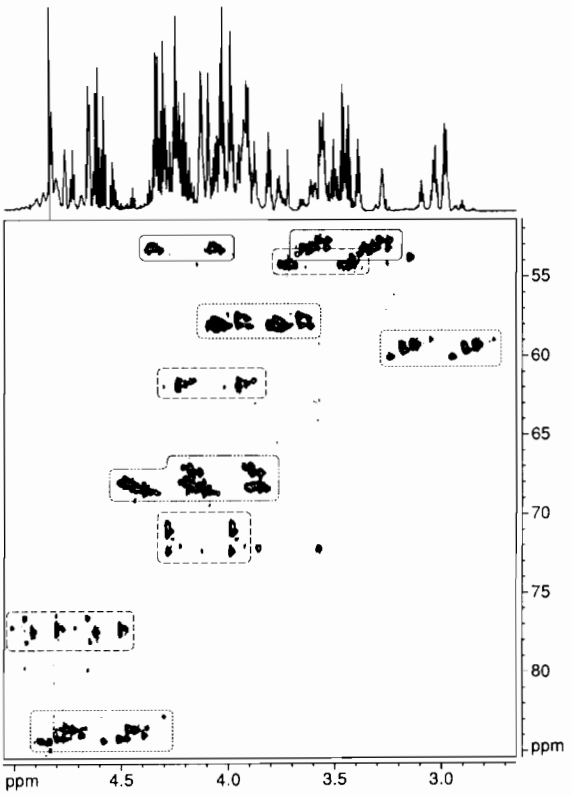

Fig. 6. $^{13}C,^{1}H$ Heteronuclear multiple quantum spectrum for $[Mo_3S_4(taci)_3]^{4+}$ (D_2O, pH 8, r.t., 11.4 Tesla, no ^{13}C decoupling during acquisition). Resonances due to the NO_2, N_2O and N_3 coordination types are indicated with boxes outlined with dashed, dotted and full lines, respectively. Overlapping regions of N_2O/N_3 resonances are circled in a dashed dotted manner.

(68.5 and 53.3 ppm). These features are commonly encountered in model complexes having the tri-amine (N_3) coordination mode.

While the above-mentioned coordination types (NO_2, N_2O and N_3) are all present in approximately equal amounts, we have no clear indication for the O_3 coordination mode. Its abundance must obviously be less than 10%.

Preparation of $[Mo_3S(S_2)_3]^{4+}$ complexes

$[Mo_3S(S_2)_3(mp)_3]Br$ has been prepared by treating $(NEt_4)_2[Mo_3S(S_2)_3Br_6]$ with an excess of the protonated ligand Hmp and a weak base (NEt_3) [5]. The product was characterized by elemental analysis and mass spectrometry (Table 2). The two ions $[Mo_3S_7mp_3]^+$ and $[Mo_3S_7mp_3 \cdot HBr]^+$, observed in the FAB mass spectrum, clearly indicated the expected replacement of the six Br^- by three bidentate mp^- ligands. The resulting complex showed a remarkably low solubility in almost every conventional solvent except DMF and DMSO.

Ligand exchange with complete preservation of the $[Mo_3S(S_2)_3]^{4+}$ core was also observed in the reaction of $[Mo_3S(S_2)_3(oxq)_3]Br$ with $Na(dtc) \cdot 3H_2O$. The complex was isolated as the dimer $[Mo_3S(S_2)_3(dtc)_3]_2S$ with a bridging sulfido group. The compound deposited in the form of brownish yellow crystals, which were hardly soluble in any solvent. In the mass spectrum, only the monomeric $[Mo_3S(S_2)_3(dtc)_3]^+$ and the corresponding fragmentation products were observed (Table 2).

Description of the structure of $[Mo_3S(S_2)_3(dtc)_3]_2S$

The dimer consists of two $[Mo_3S(S_2)_3(dtc)_3]^+$ subunits which are both linked to the bridging S(−II) via the three S_{ax} atoms of the $[Mo_3S(S_{eq}-S_{ax})_3]^{4+}$ core (Fig. 7). The bridging sulfur atom is located on a two-fold crystallographic axis and the second subunit is generated from the first by the symmetry operation $-x, 1-y, z$. A selection of summarized bond distances and bond angles is presented in Tables 6 and 7. The structure of the cluster subunit itself is closely related to those of other complexes containing the $[Mo_3S(S_2)_3(dtc)_3]^+$ moiety [5, 19], with the only exception that the $S_{eq}-S_{ax}$ bond is unusually long (Table 8). On the other hand, the distance $S_{ax}-S^{2-}$ of 2.71 Å is rather short. It should be noted that the central S^{2-} atom is not located on a center of symmetry. An angle of 33° between the two planes Mo(1)–Mo(2)–Mo(3) and Mo(1′)–Mo(2′)–Mo(3′) indicates significant deviation from coplanarity.

Discussion

The observed reactivity of $[Mo_3S(S_2)_3Br_6]^{2-}$ is summarized in Scheme 3, showing that this complex represents a versatile synthon for a variety of possible

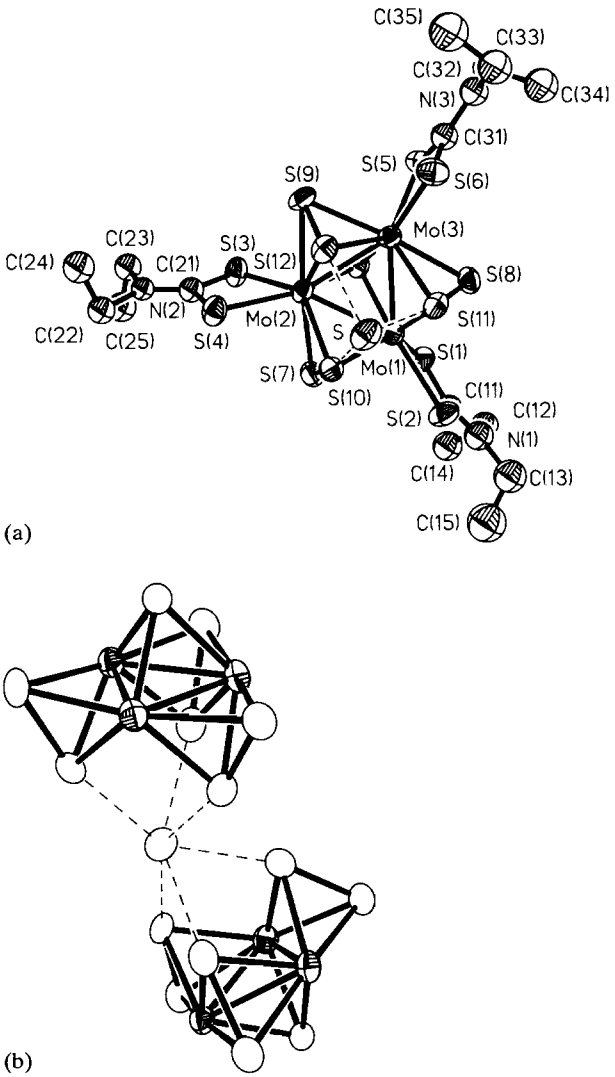

Fig. 7. Structure of the $[Mo_3S(S_2)_3(dtc)_3]_2S$ dimer. The vibrational ellipsoids are at the 50% probability level. (a) Drawing of the $[Mo_3S(S_2)_3(dtc)_3]S$ subunit with numbering scheme. (b) View of the $[Mo_3S(S_2)_3]_2S^{6+}$ core, where the open ellipsoids represent the sulfur atoms.

TABLE 6. Selected summarized interatomic distances (Å) in $[Mo_3S(S_2)_3(dtc)_3]_2S$ with e.s.d.s in parentheses

Bond	Min.	Max.	Average
Mo–Mo	2.714(3)	2.718(3)	2.716
Mo–μ_3S	2.374(6)	2.387(6)	2.381
Mo–S_{eq}	2.463(7)	2.501(7)	2.481
Mo–S_{ax}	2.409(6)	2.427(6)	2.415
Mo–S_{cis}	2.481(7)	2.495(6)	2.489
Mo–S_{trans}	2.521(7)	2.531(7)	2.526
S_{eq}–S_{ax}	2.099(9)	2.130(9)	2.113
S_{ax}–S^{2-}	2.70(1)	2.72(1)	2.71
C–S	1.68(2)	1.72(2)	1.70
C(CS_2)–N	1.34(3)	1.37(3)	1.36

TABLE 7. Summarized bond angles (°) of $[Mo_3S_7(dtc)_3]_2S$ with e.s.d.s in parentheses

Angle	Min.	Max.	Average
Mo–Mo–Mo	59.9(1)	60.1(1)	60.0
S_{ax}–Mo–S'_{ax}	81.5(2)	84.1(2)	82.9
S_{ax}–Mo–S_{eq}	50.7(2)	51.6(2)	51.1
S_{ax}–Mo–S'_{eq}	132.3(2)	135.5(2)	133.7
S_{ax}–Mo–S_{cis}	130.2(2)	134.9(2)	133.0
S_{ax}–Mo–S_{trans}	85.2(2)	88.3(2)	86.8
S_{eq}–Mo–S'_{eq}	169.4(2)	170.4(2)	169.9
S_{eq}–Mo–S_{cis}	87.6(2)	90.8(2)	89.7
S_{eq}–Mo–S_{trans}	93.1(2)	95.9(2)	94.6
S_{cis}–Mo–S_{trans}	69.5(2)	70.3(2)	69.8
μ_3S–Mo–S_{ax}	110.1(2)	111.2(2)	110.5
μ_3S–Mo–S_{eq}	83.8(2)	86.0(2)	85.0
μ_3S–Mo–S_{cis}	85.3(2)	87.5(2)	86.7
μ_3S–Mo–S_{trans}	155.5(2)	156.9(2)	156.4
Mo–S_{ax}–Mo	68.3(2)	68.6(2)	68.4
Mo–S_{ax}–S_{eq}	65.5(2)	67.0(2)	66.1
Mo–S_{eq}–Mo	66.1(2)	66.8(2)	66.4
Mo–S_{eq}–S_{ax}	62.4(2)	63.4(2)	62.8
Mo–μ_3S–Mo	69.4(2)	69.7(2)	69.5
S_{ax}–S^{2-}–S_{ax}	71.3(2)	73.1(2)	72.3
S_{ax}–S^{2-}–S'_{ax}	81.7(2)	148.7(2)	119.3

MoS cluster complexes. Fedin *et al.* [12] reported the reaction of $[Mo_3S(S_2)_3Br_6]^{2-}$ with PPh_3 and dppe, resulting in $[Mo_3S_4]^{4+}$ complexes where the phosphines and some of the Br^- ions were still coordinated to Mo, i.e. reactions where the phosphine attacked both S_{eq} and Mo. The present study demonstrates that in the presence of a suitable tridentate ligand L, Br^- and PPh_3 do not compete for coordination on Mo. Thus, the reaction $Mo_3S_7Br_6^{2-} + 3L + 3PPh_3 \rightarrow Mo_3S_4L_3^{4+} + 3S{=}PPh_3 + 6Br^-$ opens a new route for the convenient preparation of such compounds. The two complexes $[Mo_3S_4(taci)_3]^{4+}$ and $[Mo_3S_4(tdci)_3]^{4+}$, obtained in this way, are interesting models to illustrate the different ability of the two ligands for metal binding. The four different binding sites of taci give rise to a total of 20 different complexes. The total number of stereoisomers is even considerably higher, since *cis/trans* isomerism with respect to μ_3S must also be considered (Scheme 2). The present NMR study revealed indeed a high number of different species in aqueous solution of the $[Mo_3S_4(taci)_3]^{4+}$ complex. The three coordination modes, NO_2, N_2O and N_3, have been established by NMR spectroscopy. However, the O_3 coordination mode has not been observed. In the case of the tdci ligand, the N_2O and N_3 modes are disfavored for sterical reasons: the bulky dimethylamino groups impede the required chair conversion. As a consequence, only one dominant species, showing NO_2 coordination was observed in aqueous solution. Again, binding to the three oxygen atoms has not been observed. The absence of the O_3 coordination mode for both complexes – $[Mo_3S_4(taci)_3]^{4+}$ and $[Mo_3S_4(tdci)_3]^{4+}$ – indicates a preference of the $[Mo_3S_4]^{4+}$ core to coordinate, at least, one nitrogen donor atom.

The exchange of peripheral ligands under complete preservation of the $[Mo_3S(S_2)_3]^{4+}$ core has repeatedly been described for $[Mo_3S(S_2)_3Br_6]^{2-}$ [4–8]. However, it is known that the six Br atoms in $[Mo_3S(S_2)_3Br_6]^{2-}$ are much more labile than three bidentate ligands like oxq^- [39]. Since the substitution of three peripheral oxq^- ligands requires a higher energy of activation, a different reactivity of $[Mo_3S(S_2)_3Br_6]^{2-}$ and

TABLE 8. Summary of selected structural data (average distances in Å) for complexes containing the $[Mo_3S(S_2)_3]^{4+}$ core. X represents an additional anion, coordinated by the three axial sulfur atoms of the complex

Ligand	Mo–Mo	Mo–S_{eq}	Mo–S_{ax}	Mo–μ_3S	S_{eq}–S_{ax}	X	S_{ax}–X	Type[a]	f_{cov}[b]	Ref.
dtc^-	2.726	2.49	2.41	2.37	2.05	I^-	3.30	A	0.83	5
	2.708	2.48	2.41	2.38	2.06	I^-	3.25	A	0.81	5
	2.719	2.49	2.41	2.37	2.02	$TCNQ^-$ [c]	2.93	A	0.87	20
	2.721	2.48	2.41	2.37	2.04	Cl^-	3.00	A	0.82	19
	2.716	2.48	2.41	2.38	2.11	S^{2-}	2.71	B	0.73	this work
$(EtO)_2PS_2^-$	2.725	2.48	2.40	2.37	2.04	Cl^-	2.90	A	0.79	18
$Et_2PS_2^-$	2.737	2.49	2.40	2.38	2.04	Et_2PS^-	3.08	A	0.83	16
	2.730	2.48	2.40	2.37	2.05	Cl^-	2.93	A	0.80	17
						Br^-	3.05	A	0.80	17
	2.725	2.48	2.40	2.38	2.05	I^-	3.23	A	0.81	17
Cl^-	2.758	2.48	2.39	2.35	2.04	Cl^-	2.94	A	0.81	21
$Hmsa^{2-}$ [d]	2.747	2.50	2.42	2.36	2.04	Br^-	3.30	B	0.87	4
mba^{2-} [e]	2.744	2.49	2.41	2.34	2.02	COOMo[f]	2.87	A	0.88	6
$C_6H_5NH_2$, Br^-	2.730	2.48	2.39	2.36	2.05	Br^-	3.05	A	0.80	8
S_2^{2-}	2.725	2.49	2.42	2.36	2.03	$[Mo_3S_{13}]^{2-}$ [g]	3.02	A	0.82	22

[a]For definition see Chart 1. [b]$f_{cov} = d(X\text{–}S_{ax})/(r_{vdw}(X) + r_{vdw}(S))$, r_{vdw} = van der Waals' radius. [c]TCNQ = 7,7,8,8-tetracyanoquinodimethane. [d]H_3msa = 2-mercaptosuccinic acid. [e]H_2mba = 2-mercaptobenzoic acid. [f]A coordinated COO group of the ligand of an adjacent complex. [g]The μ_3S atom of an adjacent $[Mo_3(\mu_3S)(\mu_2S_2)_3(S_2)_3]^{2-}$ cluster.

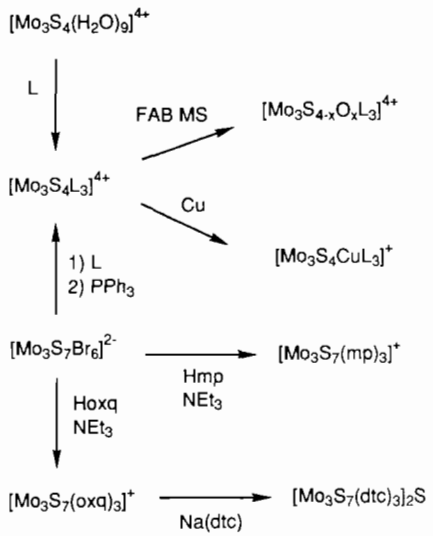

Scheme 3.

$[Mo_3S(S_2)_3(oxq)_3]^+$ must be taken into account. However, an attack of dtc^- on S_{eq}, resulting in the formation of S–dtc^-, or a deactivation of dtc^- by binding to S_{ax} has not been observed. It is a remarkable result of this study that the rather harsh reaction conditions (100 °C, 50 h, air) did not affect the $[Mo_3S(S_2)_3]^{4+}$ core at all. It is particularly interesting that S^{2-} is selectively bound to the three S_{ax} atoms. It did not coordinate to Mo nor did it react with S_{eq} (no evidence for a reaction $[Mo_3S(S_2)_3L_3]^+ + 3S^{2-} \rightarrow [Mo_3S_4L_3]^{4+} + 3S\text{–}S_{eq}{}^{2-}$ has been found).

The reactivity of the $[Mo_3S(S_2)_3]^{4+}$ core may be summarized in the following manner.

(i) The core has three distinct types of electrophilic centers: the three Mo atoms, the three S_{eq} atoms and the three S_{ax} atoms. The electrophilic nature of S_{eq} and S_{ax} is clearly established by the positive charge as revealed by Müller's SCF-Xα MO calculations [22]. Although the apical μ_3S atom is bound simultaneously to three molybdenum atoms, it must be regarded as a weak nucleophile. In Müller's $(NH_4)_2[Mo_3S_{13}]$, the apical μ_3S atom of one cluster unit is associated with the three S_{ax} atoms of an adjacent cluster core, forming infinite chains [22] (Table 8). A similar arrangement has also been found for the analogous $[Mo_3Se_{13}]^{2-}$ cluster [40].

(ii) The three electrophilic centers have a distinctly different reactivity. They interact selectively with different nucleophiles. However, it is obviously not possible to discuss this selectivity in a simple model as, for example, the HSAB correlation: the degradation of the disulfido bridges implies the transfer of the S_{eq} atoms to the nucleophile and can be understood as a reduction of S(−I) to S(−II). Consequently, the most effective agents for these reactions are strong reducing agents, i.e. soft nucleophiles. On the other hand, in a mixture of the 'soft' PPh_3 and a 'hard' tridentate ligand like tdci or taci, Mo reacts selectively with the harder nucleophile. However, the present study revealed also a complete conversion of $[Mo_3S(S_2)_3(oxq)_3]^+$ to $[Mo_3S(S_2)_3(dtc)_3]^+$, indicating a preference of the 'soft' dtc^- over the 'hard' oxq^-. There is no evidence for any mixed complex of the type $[Mo_3S(S_2)_3(oxq)_x(dtc)_{3-x}]^+$, $x=1, 2$.

(iii) A variety of different nucleophiles like Cl^-, Br^-, I^-, N-, O- and S-donors are known to interact with the anionic binding site, formed by the three S_{ax} atoms of the cluster core (Table 8). Two different structure types can be observed: the bonding of one nucleophile to one cluster unit (type A) and a dimeric structure, as described in the present paper, where one anion bridges two cluster cores (type B).

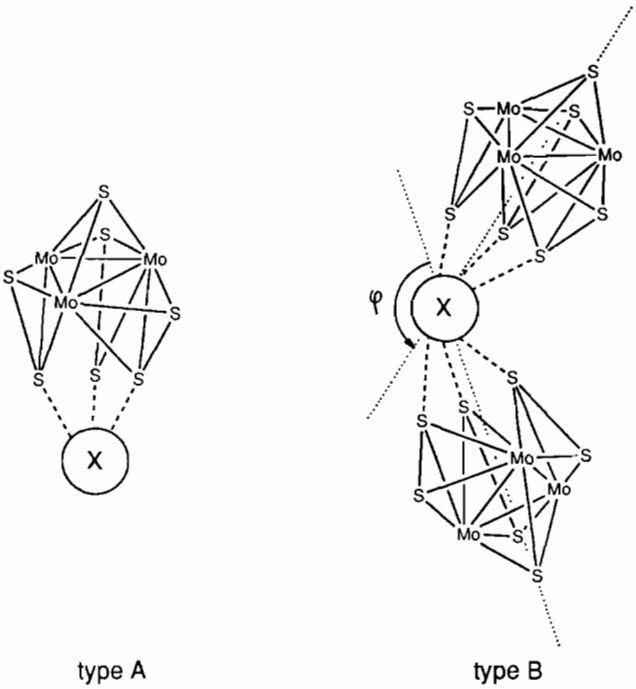

Chart 1.

In the present investigation, the type B cluster $[Mo_3S(S_2)_3(dtc)_3]_2S$ was formed by the reaction $2[Mo_3S(S_2)_3(oxq)_3]Br + 3dtc^- + S^{2-} \rightarrow [Mo_3S(S_2)_3(dtc)_3]_2S$. The source of the bridging S^{2-} atom has not been established yet. However, the hydrolysis of dtc^- (formation of $HN(Et)_2$, HS^- and CO_2) seems more likely than the decomposition of DMSO.

The nature of the anion–S_{ax} bond has been explained controversially in the literature. Covalent [18] and ionic [8] interactions have been discussed. Owing to the isolability of $S_2{}^{2-}$ and the halogens Y_2, Fedin *et al.* proposed a binding of the nucleophile X to the disulfido bridges in a similar way to that observed in the well

known adducts XY_2 [19]. For the $[Mo_3Se(Se_2)_3]^{4+}$ core, similar interactions between additional anions and the cluster core have been observed [2, 40, 41]. The observation of an inverse correlation between the Se_{ax}–anion distance and the Se_{eq}–Se_{ax} length have been interpreted as an indication for a considerable electron transfer from Se^{2-} to the cluster core [40, 41]. An analogous elongation of the S_{ax}–S_{eq} bonds has also been observed in the present $[Mo_3S(S_2)_3(dtc)_3]_2S$ (Table 9). It is also noteworthy that the S_{ax}–anion distance does not correlate with the ionic radius of the anion at all (Table 8). On the other hand, the deviation from coplanarity of the two planes Mo(1)–Mo(2)–Mo(3) and Mo(1′)–Mo(2′)–Mo(3′) in the three compounds with a type B structure varies over a wide range (Table 9). This deviation is obviously enforced by the crystal packing, indicating considerable plasticity in the coordination sphere of the central anion. The low resistance against distortion seems not quite in agreement with a predominantly covalent nature of this interaction. Considering the total charge of +0.81 on the three axial sulfur atoms [22], it becomes clear that both coulombic interactions and partial electron transfer are significantly involved in this bonding.

Nothing is known about the binding energy of such S_{ax}–anion interactions. The observation that the mass spectra of a variety of complexes, where such interactions have been verified by X-ray analysis, showed only a peak of the dissociated $[Mo_3S(S_2)_3L_3]^+$ entity [5, 17], does not necessarily imply a weak binding of the anion. In most of these complexes, the coordination of a mononegative ligand L^- resulted in a monopositive complex $[Mo_3S(S_2)_3L_3]^+$ and a neutral adduct $[Mo_3S(S_2)_3L_3]X$. Since proton uptake of the ligand L or oxidation of the cluster core can hardly occur in these complexes, a monopositive adduct is not available and is therefore not visible in the spectrum. To elucidate the stability of the adduct under FAB conditions, $[Mo_3S(S_2)_3(mp)_3]Br$ has been prepared. In this complex, the coordinated ligand may easily be protonated. As a consequence, two individual peaks, assignable to $[Mo_3S_7mp_3]^+$ and $[Mo_3S_7mp_3 \cdot HBr]^+$, were indeed visible in the spectrum.

TABLE 9. Structural data of dimeric $[Mo_3Y_7L_3]_2X$ (type B) clusters. Y: S, Se; L: bidentate ligand; X: additional anion

Complex	X	φ[a]	f_{cov}[b]	f_{elong}[c]	Ref.
$H_5[Mo_3S(S_2)_3(msa)_3]_2Br^{6-}$	Br	180	0.87	0.99	4[d]
$[Mo_3S(S_2)_3(dtc)_3]_2S$	S	147	0.73	1.02	this work
$[Mo_3Se(Se_2)_3(Se_2)_3]Se$	Se	139	0.74	1.02	40

[a]For definition, see Chart 1. [b]$f_{cov} = d(X–Y_{ax})/(r_{vdw}(X) + r_{vdw}(Y))$, r_{vdw} = van der Waals' radius. [c]$f_{elong} = d(Y_{eq} - Y_{ax})/d(Y–Y)_{elem}$. [d]$H_3msa$ = 2-mercaptosuccinic acid.

Acknowledgements

We thank Beat Müller for recording NMR spectra, Rolf Häfliger for measurements of the mass spectra and Thomas Kradolfer for performing the X-ray experiments and for revising the manuscript. We are indebted to Dr Valdimir Fedin for interesting discussions. Financial support of the Schweizerischer Nationalfonds zur Förderung der wissenschaftlichen Forschung (Project No. 21-30773-91) for M.M. is gratefully acknowledged.

References

1 (a) S.C. Lee and R.H. Holm, *Angew. Chem., 102* (1990) 868, and refs. therein; (b) V.P. Fedin, M.N. Sokolov, K.G. Myakishev, O.A. Geras'ko and V.Ye. Fedorov, *Polyhedron, 10* (1991) 1311; (c) V.P. Fedin, M.N. Sokolov, O.A. Geras'ko, B.A. Kolesov and V.Ye. Fedorov, *Inorg. Chim. Acta, 175* (1990) 217; (d) F.A. Cotton, P.A. Kibala and C.S. Miertschin, *Inorg. Chem., 30* (1991) 548; (e) A. Müller, V. Fedin, K. Hegetschweiler and W. Amrein, *J. Chem. Soc., Chem. Commun.,* (1992) 1795.
2 V.P. Fedin, M.N. Sokolov, O.A. Geras'ko, A.V. Virovets, N.V. Podberezskaya and V.Ye. Fedorov, *Inorg. Chim. Acta, 187* (1991) 81.
3 F.A. Cotton, P.A. Kibala, M. Matusz, C.S. McCaleb and R.B.W. Sandor, *Inorg. Chem., 28* (1989) 2623.
4 K. Hegetschweiler, T. Keller, H. Zimmermann, W. Schneider, H. Schmalle and E. Dubler, *Inorg. Chim. Acta, 169* (1990) 235.
5 H. Zimmermann, K. Hegetschweiler, T. Keller, V. Gramlich, H. Schmalle, W. Petter and W. Schneider, *Inorg. Chem., 30* (1991) 4336.
6 K. Hegetschweiler, T. Keller, M. Bäumle, G. Rihs and W. Schneider, *Inorg. Chem., 30* (1991) 4342.
7 V.P. Fedin, M.N. Sokolov, O.S. Kibirev, A.V. Virovets, N.V. Podberezskaya and V.E. Fedorov, *Russ. J. Inorg. Chem., (Engl. Transl.), 36* (1991) 1735.
8 V.P. Fedin, Y.V. Mironov, A.V. Virovets, N.V. Podberezskaya and V.Ye. Fedorov, *Polyhedron, 11* (1992) 2083.
9 (a) H. Keck, W. Kuchen, J. Mathow, B. Meyer, D. Mootz and H. Wunderlich, *Angew. Chem., 93* (1981) 1019; (b) F.A. Cotton and R. Llusar, *Polyhedron, 6* (1987) 1741; (c) T. Shibahara, M. Yamasaki, G. Sakane, K. Minami, T. Yabuki and A. Ichimura, *Inorg. Chem., 31* (1992) 640.
10 T. Shibahara and H. Kuroya, *Polyhedron, 5* (1986) 357.
11 F.A. Cotton, Z. Dori, R. Llusar and W. Schwotzer, *Inorg. Chem., 25* (1986) 3654.
12 V.P. Fedin, M.N. Sokolov, Yu.V. Mironov, B.A. Kolesov, S.V. Tkachev and V.Ye. Fedorov, *Inorg. Chim. Acta, 167* (1990) 39.
13 F.A. Cotton, R.L. Luck and C.S. Miertschin, *Inorg. Chem., 30* (1991) 1155.
14 (a) A. Müller and U. Reinsch, *Angew. Chem., 92* (1980) 69; (b) T.R. Halbert, K. McGauley, W.-H. Pan, R.S. Czernuszewicz and E.I. Stiefel, *J. Am. Chem. Soc., 106* (1984) 1849; (c) H. Keck, W. Kuchen, J. Mathow and H. Wunderlich, *Angew. Chem., 94* (1982) 927.

15 (a) V.P. Fedin, B.A. Kolesov, Yu.V. Mironov and V.Ye. Fedorov, *Polyhedron, 8* (1989) 2419; (b) K. Hegetschweiler, P. Caravatti, V.P. Fedin and M.N. Sokolov, *Helv. Chim. Acta, 75* (1992) 1659.

16 B. Meyer and H. Wunderlich, *Z. Naturforsch., Teil B, 37* (1982) 1437.

17 G. Borgs, H. Keck, W. Kuchen, D. Mootz, R. Wiskemann and H. Wunderlich, *Z. Naturforsch., Teil B, 46* (1991) 1525.

18 M. Shang, J. Huang and J. Lu, *Acta Crystallogr., Sect. C, 40* (1984) 759.

19 V.P. Fedin, M.N. Sokolov, O.A. Geras'ko, A.V. Virovets, N.V. Podberezskaya and V.Ye. Fedorov, *Inorg. Chim. Acta, 192* (1992) 153.

20 V.P. Fedin, M.N. Sokolov, A.V. Virovets, N.V. Podberezskaya and V.Ye. Fedorov, *Inorg. Chim. Acta, 194* (1992) 195.

21 P. Klingelhöfer, U. Müller, C. Friebel and J. Pebler, *Z. Anorg. Allg. Chem., 543* (1986) 22.

22 A. Müller, V. Wittneben, E. Krickemeyer, H. Bögge and M. Lemke, *Z. Anorg. Allg. Chem., 605* (1991) 175–188.

23 J. Jeener, B.H. Meier, P. Bachmann and R.R. Ernst, *J. Chem. Phys., 71* (1979) 4546.

24 A. Bax and D.G. Davis, *J. Magn. Reson., 65* (1985) 355.

25 (a) A. Bax and S. Subramanian, *J. Magn. Reson., 67* (1986) 565; (b) A. Bax and M.F. Summers, *J. Am. Chem. Soc., 108* (1986) 2093.

26 M. Ghisletta, H.-P. Jalett, T. Gerfin, V. Gramlich and K. Hegetschweiler, *Helv. Chim. Acta, 75* (1992) 2233.

27 K. Hegetschweiler, I. Erni, W. Schneider and H. Schmalle, *Helv. Chim. Acta, 73* (1990) 97.

28 F.A. Cotton, Z. Dori, R. Llusar and W. Schwotzer, *J. Am. Chem. Soc., 107* (1985) 6734.

29 K. Korzekwa, W.N. Howald and W.F. Trager, *Biomed. Environ. Mass Spectrom., 19* (1990) 211.

30 G.M. Sheldrick, *SHELXTL-Plus 88,* structure determination software programs, Nicolet Instrument Corp., Madison, WI, 1988.

31 T. Shibahara, H. Akashi and H. Kuroya, *J. Am. Chem. Soc., 110* (1988) 3313.

32 Q.-T. Liu, J. Lu and A.G. Sykes, *Inorg. Chim. Acta, 198–200* (1992) 623.

33 K. Hegetschweiler, V. Gramlich, M. Ghisletta and H. Samaras, *Inorg. Chem., 31* (1992) 2341.

34 K. Hegetschweiler, R.D. Hancock, M. Ghisletta, T. Kradolfer, V. Gramlich and H.W. Schmalle, *Inorg. Chem.,* in press.

35 K. Hegetschweiler, M. Ghisletta, T.F. Fässler, R. Nesper, H.W. Schmalle and G. Rihs, *Inorg. Chem., 32* (1993) 2032–2041.

36 K. Hegetschweiler, M. Ghisletta, T. Kradolfer, H.W. Schmalle and V. Gramlich, manuscript in preparation.

37 L. Haushcrr-Primo, M. Ghisletta, V. Gramlich and K. Hegetschweiler, manusript in preparation.

38 K. Hegetschweiler, M. Ghisletta and V. Gramlich, *Inorg. Chem., 32* (1993) 2699–2704.

39 K. Hegetschweiler, T. Keller, W. Amrein and W. Schneider, *Inorg. Chem., 30* (1991) 873.

40 J.-H. Liao and M.G. Kanatzidis, *Inorg. Chem., 31* (1992) 431.

41 J.-H. Liao and M.G. Kanatzidis, *J. Am. Chem. Soc., 112* (1990) 7400.